

AstroBox2 – Detector for low-energy β -delayed particle detection



A. Saastamoinen^{a,*}, E. Pollacco^b, B.T. Roeder^a, A. Spiridon^a, M. Daq^a, L. Trache^c, G. Pascovici^c, R. De Oliveira^d, M.R.D. Rodrigues^e, R.E. Tribble^a

^a Cyclotron Institute, Texas A&M University, College Station, TX 77843, USA

^b IRFU, CEA Saclay, Gif-sur-Yvette, France

^c National Institute of Physics and Nuclear Engineering, Bucharest-Magurele RO-077125, Romania

^d CERN, Geneva, Switzerland

^e Instituto de Física, Universidade de São Paulo, Caixa Postal 66318, CEP 05314-970, São Paulo, SP, Brazil

ARTICLE INFO

Article history:

Received 2 September 2015

Received in revised form 4 February 2016

Accepted 4 February 2016

Available online 12 March 2016

Keywords:

Radioactive ion beams

Micro pattern gas amplifier detector

MPGAD

Implantation

$\beta\beta$ $\beta\gamma$

ABSTRACT

Efficient suppression of β -background is essential for studies of low-energy β -delayed charged particle decays of astrophysical interest. A promising method for such studies has been a micro pattern gas amplifier detector where the sample is implanted into the gas volume and the decays that follow are observed with high gain and signal to noise ratio. An upgraded version of the original AstroBox detector has been built and commissioned at Texas A&M University. Here a description of the new AstroBox2 detector is given, selected results from the commissioning tests are presented, and future perspectives discussed.

© 2016 Elsevier B.V. All rights reserved.

1. Introduction

Resonant reactions are important in many explosive hydrogen-burning scenarios. The key parameters in understanding the aforementioned astrophysical reaction rates are the energies and decay widths of the associated nuclear states along the reaction paths. The relevant states for particle capture reactions are located in the Gamow window, just above the associated particle separation threshold (e.g. proton separation energy, S_p). The properties of these states can be probed by using indirect methods, which include β -decay studies.

Over the past years we have studied the decay of several beta-delayed proton emitters of astrophysical interest by implanting the nuclei of interest into Si detectors of various segmentations [1–5]. In these studies it was realized that shrinking the physical detection volume of elements in a Si detector does not reduce the beta-background to allow unambiguous interpretation of the proton data originating from weak decay branches in the typical energy range of astrophysically interesting decays ($E_p \sim$ few hundred keV). To further reduce the β -background a novel gas detector, AstroBox was developed [6]. The Astrobox detector is based

on Micro Pattern Gas Amplifier Detector (MPGAD) technology [7] and was proven to work in operating conditions required for low energy β -delayed charged particle detection.

We have built an upgraded version of this detector, AstroBox2. The major change to the first version [6] is the overall size and change of the segmentation geometry of the MPGAD anode. The earlier cylindrical symmetry with only five segments has been replaced by a set of 29 rectangular anode pads that are arranged into a symmetric geometry along the beam axis. The new configuration allows better control of the source implantation and gives more refined possibilities for decay studies. The new custom made detector chamber has several technical improvements that enhance the overall usability of the setup. In this article we give a description of the AstroBox2 detector and results from the first commissioning tests.

2. Description of the detector

The general operating principle of the detector and associated components is similar to the description in Ref. [6]. In short, AstroBox2 detector, shown in Fig. 1, is a rectangular-shaped gas detector, operated in a mode in which the ions of interest are stopped inside the gas volume and let decay. The electrons created by the decay radiation ionizing the gas are drifted towards a gas

* Corresponding author. Tel.: +1 979 845 1411; fax: +1 979 845 1899.

E-mail address: ajsaasta@comp.tamu.edu (A. Saastamoinen).

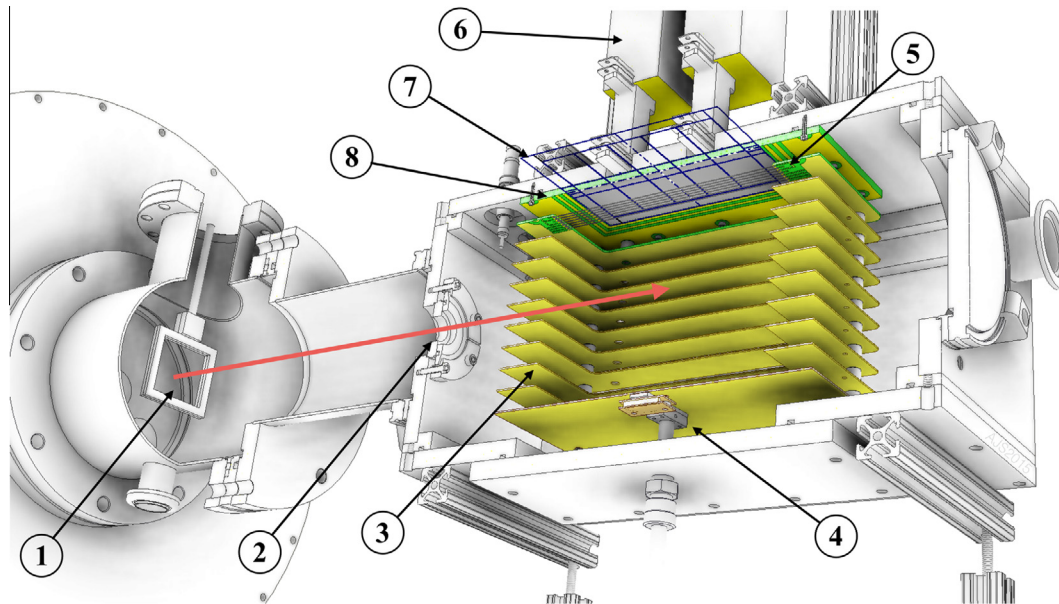


Fig. 1. An illustration of the AstroBox2 detector setup. The red arrow indicates secondary beam direction from the MARS spectrometer. (1) Rotatable degrader frame. (2) Aramite window (50 μm) separating gas volume from separator vacuum. (3) Field cage equipotential rings. (4) Cathode with a source holder that can be masked while the detector remains under operating conditions. (5) Gating grid. (6) Preamplifiers. (7) An overlaid grid highlighting the Micromegas detector anode pad structure, cf. Fig. 4. (8) The PCB onto which the Micromegas is mounted. See text for more details. (For interpretation of the references to color in this figure legend, the reader is referred to the web version of this article.)

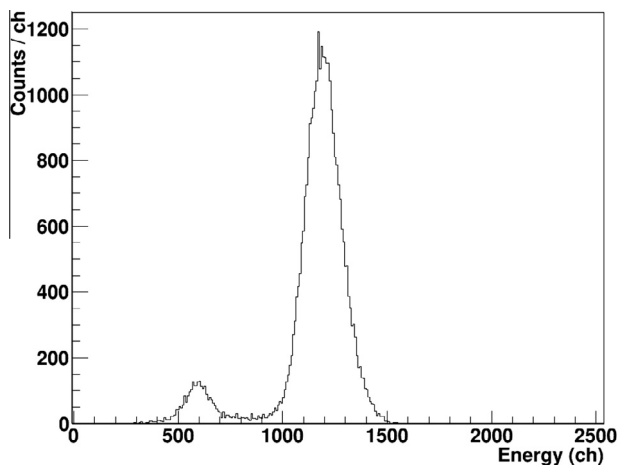


Fig. 2. Detector response to ^{55}Fe X-ray source. Typical resolution of 14–16% is achieved for the 5.9 keV X-ray when taking into account the weaker 6.5 keV X-ray distorting the shape. The small peak on left is the Ar X-ray escape peak.

amplifier based on Micromegas technology [7]. The Micromegas detector element with active area of 100 mm \times 145 mm is divided into 29 rectangular anode pads of various sizes arranged symmetrically along the beam axis. At the moment only a detector with a 128- μm amplification gap has been tested, but we have acquired also detectors with 256 μm and 64 μm gaps. The pad layout is shown in Figs. 1 and 4. The detector printed circuit board (PCB) doubles as a sub-flange which allows the signals to be transmitted directly to the readout electronics and the detector element voltages to be applied without any feed-throughs.

The signals from the 29 anode pads are read out with two Mesytec MPR16-100 16 channel preamplifiers coupled to Mesytec MSCF16 shaper/discriminator modules. The detector is triggered as a logic OR of any of the pads. The data acquisition consists of one Mesytec 32 channel MADC32 ADC in 8 k hi-res mode for energy

information, a CAEN V1190A TDC for timing information, and two of Struck Innovative Systeme SIS3820 scalers for rate monitoring and decay time measurements.

The field cage with spacing of 16.5 mm is mounted on the detector PCB. The rest of the chamber was designed around the detector assembly by keeping the size as small as possible, while taking into account the minimal safe distance to run the cathode at a potential of -3.3 kV to achieve a uniform electric field of about 200 V/cm across the whole active gas volume. The equipotential

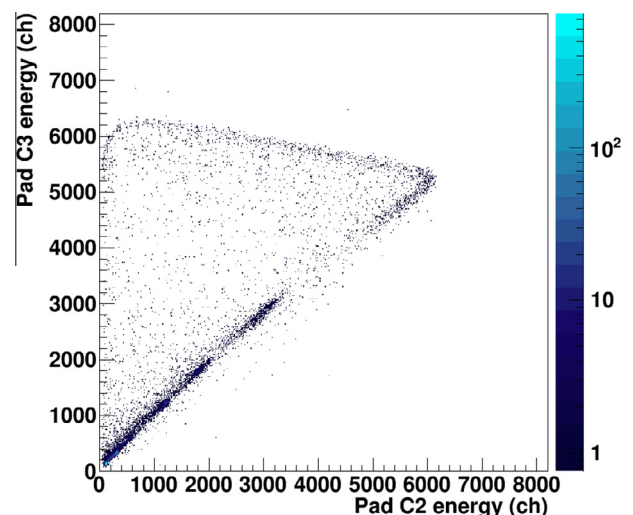


Fig. 3. Measured energy losses in two pads (labeled C2,C3) along the beam path versus each other when the ^{25}Si beam is stopped on the pad C3 (the centermost pad of the detector). The diagonal has the ions with same magnetic rigidity and $Z < 14$ punching through these two pads. The almost horizontal line indicates the energy loss of ^{25}Si particles stopping in different locations within the pad C3. The fraction of ^{25}Si ions punching through the following pad (C4, not shown) are located in the corner formed by the diagonal and the horizontal line.

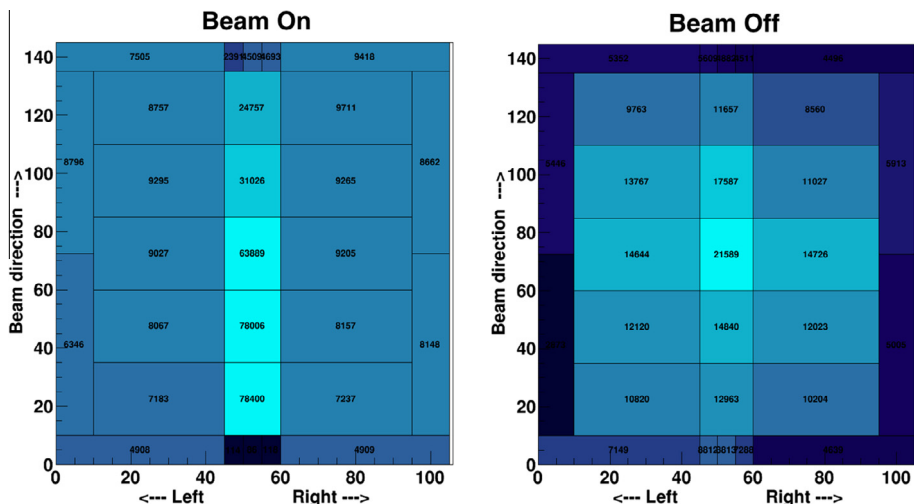


Fig. 4. Event display showing the anode pads with signal above set threshold. Data from same run as in Fig. 3. The axis units are in mm, corresponding to the physical detector layout, cf. Fig. 1. When the beam is on (left panel), the majority of signal is collected from the centermost pad, and from the pads along the beam axis. When beam is switched off (right panel) the most intense counts (brighter color) are confined into the centermost pad where the beam has stopped and where majority of decays occur.

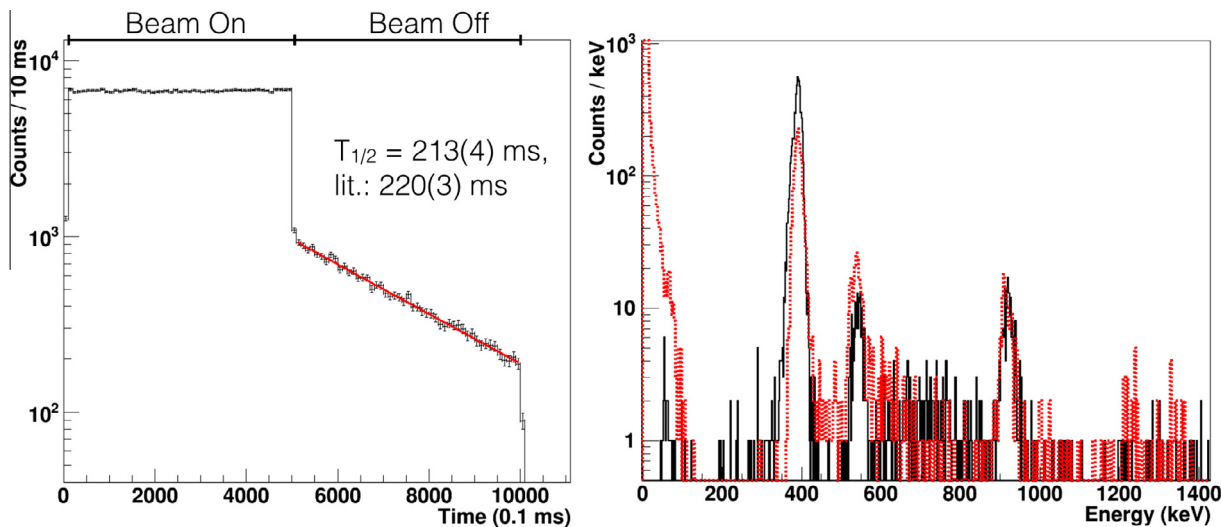


Fig. 5. Left: Decay time spectrum of ^{25}Si gated by the decay energies of the 401, 555, and 943 keV proton peaks. The data was collected during beam off period of a pulsed beam with a cycle of 500 ms on and 500 ms off. Right: Measured β -delayed proton spectrum of ^{25}Si (black, solid) compared to a GEANT4 simulation (red, dashed) when decays are confined into one pad active volume. The experimental data is cut at about 100 keV due to the discriminator threshold, whereas the simulation shows the expected background without electronics threshold. Resolution of the 401 keV proton group is $\sim 4\%$. (For interpretation of the references to color in this figure legend, the reader is referred to the web version of this article.)

ring closest to the Micromegas is a PCB having a set of 50 μm thick wires, forming a gating grid that can be used to limit the transmission of the drifting electrons. All high voltages for the anode pads and for the gating grid were taken from Ortec 710 bias supply (0–1 kV) or Mesytec MHV4 (0–400 V), and the cathode voltage was provided from Ortec 549 bias supply (0–5 kV).

The overall construction of the chamber is modular, allowing easy customization for different experimental needs. All materials inside the gas volume are chosen to be minimally outgassing, and all hardware inside the gas volume is of vented design by default. At the moment the gas handling system is the same as in AstroBox [6]. There are two variants of the cathode. The first is solid construction with a source holder in which the test source can be masked without breaking the vacuum. The second cathode is a thin copper mesh soldered on a spare field cage element. This transparent construction allows scanning of the whole active detector area by a movable source holder.

3. Source tests

The first detector element with 128 μm amplification gap has been tested off-line in various conditions to determine operational parameters for optimal performance. All tests were carried out using a P5 gas mixture (5% CH_4 + 95% Ar) at 800 torr pressure, which is a typical pressure required for β -delayed proton decay studies. In all off-line and on-line tests the cathode was run at -3.3 kV, the mesh was kept at ground potential, and the anode voltage was varied to adjust the gas gain.

The detector response for α sources was tested with a mixed source containing ^{148}Gd , ^{239}Pu , ^{241}Am , and ^{244}Cm . The source is housed in a tightly collimated holder (two 1 mm holes 3 mm apart) over the centermost anode pad. Typical resolution of 3% is achieved for the 5.486 MeV ^{241}Am α line.

An extensive set of tests was carried out with an ^{55}Fe X-ray source by utilizing the transparent cathode. The collimated X-ray

source was mounted on a steel ring sitting on a plexiglass window at the bottom of the chamber. This configuration allows moving the source with a magnet outside the window, while keeping the detector under operational conditions (magnet can be removed to avoid distortion of the field inside the detector). The response of the centermost pad to the 5.9 keV X-ray is shown in Fig. 2. Typical resolution of 14–16% is achieved across the whole detector.

4. In-beam test with β p-decay of ^{25}Si

The in-beam test was conducted at the Cyclotron Institute of Texas A&M University. A secondary beam of ^{25}Si was produced through fragmentation by bombarding a 254 μm thick Al foil with a 40-MeV/u ^{28}Si beam from the K500 cyclotron. The reaction products were separated with the Momentum Achromat Recoil Spectrometer (MARS) [8], yielding a beam of ^{25}Si with 25% purity at 34 MeV/u and $\delta p/p = 0.25\%$. During the testing, a typical implantation rate was about 50 pps for ^{25}Si .

To implant the sample into the detector, the beam was passed through a rotatable 21 mil (533 μm) thick Al degrader and through a 50 μm thick aramica window. The combination of small initial momentum distribution and adjustable degrader thickness allows precise control of implantation of the sample over the desired pad. As all species in the beam from MARS have same magnetic rigidity, the relatively low density of the stopping medium lets the impurities with lower Z pass through the active volume of the detector, whereas impurities with higher Z are stopped before reaching the active volume. The beam energy loss of two pads versus each other along the beam path is shown in Fig. 3 for the case when the beam stops over the centermost pad of the detector. For more detailed description of the implantation procedure, see Ref. [6]. In this configuration the gating grid was kept at the corresponding field cage potential of -330 V , whereas the anode voltage was at $+300\text{ V}$ to limit amplification of the large signal induced by the beam.

In the measurement configuration, the gating grid was pulsed between ground (beam on) and the corresponding field cage potential of about -330 V (beam off). The high voltage pulsing was done by using a Behlke HTS-31-03-GSM switch that was synchronized to the cyclotron beam pulsing. The beam on and off periods were both 500 ms with 5 ms wait period in-between to allow settling of the gating grid voltage transition induced noise. The anode was run at $+450\text{ V}$.

Fig. 4 illustrates event display for both beam on and off cases when the beam is stopped into the centermost pad and following decays observed. A sample of the observed β -delayed proton spectrum and associated time spectrum is shown in Fig. 5. The energy

spectrum shown is generated by vetoing all the surrounding pads around the pad where the beam was stopped on. In this way, the β -background of the measured data is suppressed below the used discriminator threshold of about 100 keV (simulated spectrum shows the expected background without electronics threshold). A comparison of the measured data to a GEANT4 [9] simulation, based on the energies and branching ratios of the latest decay study of Thomas et al. [10] shows a reasonably good agreement. The difference in intensities is likely due to fact that these proton groups were on top of large β -background in Ref. [10].

5. Future developments and outlook

So far the very first detector element with 128 μm amplification gap has been thoroughly tested. We have recently acquired two new detector elements using a more uniform, electroformed mesh with amplification gaps of 64 and 128 μm . These will be tested during fall 2015 and spring 2016. Future improvements of the detector under consideration include replacing the old gas handling system with an improved new system including fully electropolished stainless steel tubing, added filters, and fully oil free pumping for more reliable and faster gas handling. Other future additions for the setup will include HPGe detectors for identifying possible particle- γ -coincidences to distinguish whether the observed particles populate the ground state or some excited state in the proton daughter. In addition, an implementation of digital GET (General Electronics for TPCs) electronics for the data readout is under consideration. The first physics runs are foreseen to be conducted during spring 2016.

Acknowledgements

This work has been supported in part by the US DOE under Grants DE-FG02-93ER40773 and DE-NA0001786, and by the grant PN2-ID-27-2013 from ANCSI Bucharest, Romania. Authors thank Praveen Schidling for lending the Behlke HV switch for the test run.

References

- [1] A. Saastamoinen et al., *Phys. Rev. C* 83 (4) (2011) 045808.
- [2] L. Trache, et al., *PoS(NIC X)* (2008) 163.
- [3] A. Saastamoinen et al., *AIP Conf. Proc.* 1409 (4) (2011) 71.
- [4] J. Wallace et al., *Phys. Lett. B* 712 (1–2) (2012) 59–62.
- [5] M. McCleskey et al., *Nucl. Instr. Meth. Phys. Res. A* 700 (2013) 124.
- [6] E. Pollacco et al., *Nucl. Instr. Meth. Phys. Res. A* 723 (2013) 102.
- [7] Y. Giomataris et al., *Nucl. Instr. Meth. Phys. Res. A* 376 (1) (1996) 29–35.
- [8] R. Tribble et al., *Nucl. Phys. A* 701 (1–4) (2002) 278–281.
- [9] S. Agostinelli et al., *Nucl. Instr. Meth. Phys. Res. A* 506 (3) (2003) 250–303.
- [10] J.-C. Thomas et al., *Eur. Phys. J. A* 21 (2004) 419–435.